PRAMANA
— journal of
physics

Vol. 78, No. 2
February 2012
pp. 247–255

Physics design of a CW high-power proton Linac for accelerator-driven system

RAJNI PANDE*, SHWETA ROY, S V L S RAO, P SINGH and S KAILAS
Physics Group, Bhabha Atomic Research Centre, Mumbai 400 085, India
*Corresponding author. E-mail: pande_rajni@rediffmail.com

MS received 5 April 2011; revised 15 June 2011; accepted 15 July 2011

Abstract. Accelerator-driven systems (ADS) have evoked lot of interest the world over because of their capability to incinerate the MA (minor actinides) and LLFP (long-lived fission products) radiotoxic waste and their ability to utilize thorium as an alternative nuclear fuel. One of the main subsystems of ADS is a high energy (∼1 GeV) and high current (∼30 mA) CW proton Linac. The accelerator for ADS should have high efficiency and reliability and very low beam losses to allow hands-on maintenance. With these criteria, the beam dynamics simulations for a 1 GeV, 30 mA proton Linac has been done. The Linac consists of normal-conducting radio-frequency quadrupole (RFQ), drift tube linac (DTL) and coupled cavity drift tube Linac (CCDTL) structures that accelerate the beam to about 100 MeV followed by superconducting (SC) elliptical cavities, which accelerate the beam from 100 MeV to 1 GeV. The details of the design are presented in this paper.

Keywords. Radio-frequency quadrupole; drift tube Linac; coupled cavity drift tube Linac; superconducting elliptical cavity; high intensity proton Linac; accelerator-driven subcritical reactor system.

PACS Nos 29.20.Ej; 29.27.−a; 29.27.Bd

1. Introduction

High-power proton accelerators have various applications as accelerator-driven systems (ADS), spallation neutron sources, next-generation radioactive ion beam facilities, neutrino factories etc. The accelerator-driven system [1] consists of a subcritical reactor that is driven by an external neutron source produced by a high-power proton beam hitting a high Z material and producing neutrons by spallation. Accelerator-driven systems have the capability to incinerate MA (minor actinides) and LLFP (long-lived fission products) radiotoxic waste and can utilize both uranium and thorium as nuclear fuel and produce energy without producing much radioactive wastes. This is of particular interest to India's nuclear programme due to its vast thorium resources [2]. The main components of ADS are: a high-power proton accelerator (1 GeV, 10's of mA current), spallation target (heavy elements like Pb, W, U, ...) and a sub-critical reactor.

DOI: 10.1007/s12043-011-0220-2; ***e*Publication: 10 January 2012**

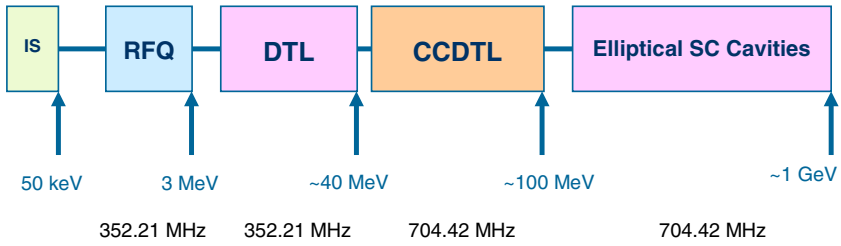

Figure 1. Lay-out of the 1 GeV Linac.

The accelerator for ADS is required to deliver proton beam of up to several tens of MW power and operate in the CW mode with high-intensity beams. At present there is no such operating machine in the world. The SNS [3] at Oak Ridge, USA, a Linac-based spallation neutron source, is the highest power operating machine in the pulsed mode at 1.4 MW.

The high-power Linac essentially consists of low-energy, the intermediate-energy and the high-energy sections. The low-energy section consists of a high-intensity ion source that delivers beams of few tens of keV energy. Almost all Linacs being designed today use the radio-frequency quadrupole (RFQ) [4,5] to accelerate the high current beam from the ion source to a few MeV beam energy. The intermediate-energy structures accelerate the beam to about 100 MeV. These structures are usually normal-conducting drift-tube Linac structures (DTL, SDTL, CCDTL) [6,7]. However, superconducting structures, like spoke-type resonators, are also being contemplated especially for CW beams [8]. The high-energy structures accelerate the beams from few hundred MeV to GeV energies. At these energies, superconducting RF technology seems to be the best option in order to design a cost-effective machine in terms of both capital and operational costs. Superconducting multicell elliptical cavities [9] are used for acceleration.

In India, it is planned that the development of the 1 GeV accelerator for ADS will be pursued in three phases, namely, 20 MeV, 100 MeV and 1 GeV. In the first stage, a low-energy high-intensity proton accelerator (LEHIPA) is being built in BARC, India as the front end injector to the Linac for ADS [10]. An accelerator configuration for a 1 GeV, 30 mA Linac has been worked out and the physics design studies have been done in detail. The main design criterion for such a Linac is the beam loss (<1 W/m) in the accelerator to allow hands-on-maintenance of the entire Linac. The Linac consists of normal-conducting radio-frequency quadrupole (RFQ), drift tube Linac (DTL) and coupled cavity drift tube Linac (CCDTL) structures that accelerate the beam to about 100 MeV followed by super-conducting (SC) elliptical cavities, which accelerate the beam from 100 MeV to 1 GeV. The lay-out of the 1 GeV Linac is shown in figure 1.

2. Linac design

The Linac has a normal conducting front-end that accelerates the 30 mA, CW proton beam to 100 MeV followed by a high-energy superconducting Linac section that accelerates the beam to 1 GeV. The front end consists of a 3 MeV RFQ, DTL upto 40 MeV and CCDTL upto 100 MeV while the high-energy Linac is made up of 5 cell superconducting elliptical cavities of 3 different types. The RFQ and DTL operate at 352.21 MHz and the CCDTL

and SC Linac operate at the second harmonic frequency at 704.42 MHz. The transverse and longitudinal phase advances per unit length are maintained constant at all transitions between the structures to provide a current independent match into the next structure [11]. For this, the quadrupole gradients and accelerating electric fields are varied between the structures.

The ion source will be an ECR ion source that can deliver upto 40 mA proton beam at 50 keV energy. A low-energy beam transport (LEBT) line is used to match and transport this beam into RFQ. The matching is done using two solenoids. The 4-vane CW RFQ [12] operating at 352.21 MHz will accelerate the beam from 50 keV to 3 MeV. The RFQ has been designed for a constant vane voltage of 76.7 kV. With this the peak electric field is limited to 1.8 times the Kilpatrick limit. The transmission at the end of the RFQ is 95.9%. The parameters of the RFQ are shown in table 1. The total length of the RFQ is 3.52 m and the total RF power requirement is 385 kW which includes 88.5 kW of beam power.

The 3 MeV beam from the RFQ is then matched into the DTL using a matching line (MEBT), which consists of four quadrupoles for transverse matching and two RF buncher cavities for longitudinal matching. The beam from the RFQ is accelerated to 40 MeV using a 352.21 MHz DTL. A FFDD lattice is used in the DTL for transverse focussing. For this lattice the quadrupole gradient required to match the transverse phase advance between RFQ and DTL for current independent matching works out to be 43 T/m. The focussing lattice period is $4\beta\lambda$ throughout the DTL. The total length of the DTL is 28 m and the RF power required is 3 MW. The axial electric field is kept constant at 2.5 MV/m in all the tanks.

The 40 MeV beam from the DTL is then accelerated to 100 MeV using 2-gap CCDTL cavities at 704.42 MHz. An important figure of merit used to characterize an accelerating cavity is the effective shunt impedance per unit length. It is a measure of the energy gain per unit power dissipation and is defined as

$$ZT^2 = \frac{(E_0 T)^2}{P/L},$$

where E_0 is the average axial electric field, T is the transit time factor, P is the average power dissipation and L is the length of the cavity.

Table 1. Parameters of the RFQ.

Parameters	Value
Frequency	352.21 MHz
Input energy	50 keV
Output energy	3 MeV
Input current	30 mA
Transverse emittance	0.02/0.023 π cm-mrad
Synchronous phase	$-30°$
Vane voltage	76.7 kV
Peak surface field	32.51 MV/m
Length	3.52 m
Total RF power	385 kW
Transmission	95.9%

The accelerating structures are optimized for maximum effective shunt impedance per unit length and minimum power dissipation using the SUPERFISH code. At 40 MeV, it was found that the effective shunt impedance of the CCDTL starts becoming more than that of the DTL and the power dissipation in the two structures is comparable as can be seen from figure 2. Hence at 40 MeV, we have switched to 2-gap CCDTL structure at 704.42 MHz.

Each CCDTL cavity contains a single drift tube inside mounted by stems and electromagnetic quadrupoles are mounted between two CCDTL cavities for transverse focussing. The transverse focussing lattice is FD and the focussing period is $5\beta\lambda$ at this frequency. The beam from the DTL is transversely matched into the CCDTL using the first four quadrupoles in the CCDTL. The accelerating gradient is initially kept low at 1.04 MV/m for matching longitudinal phase advance per unit length between the DTL and CCDTL. It is then gradually increased from 1.04 MV/m to 2.5 MV/m to decrease the overall length of the CCDTL. Its total length is about 70 m and the RF power requirement is 6.5 MW. The main parameters of DTL and CCDTL are given in table 2.

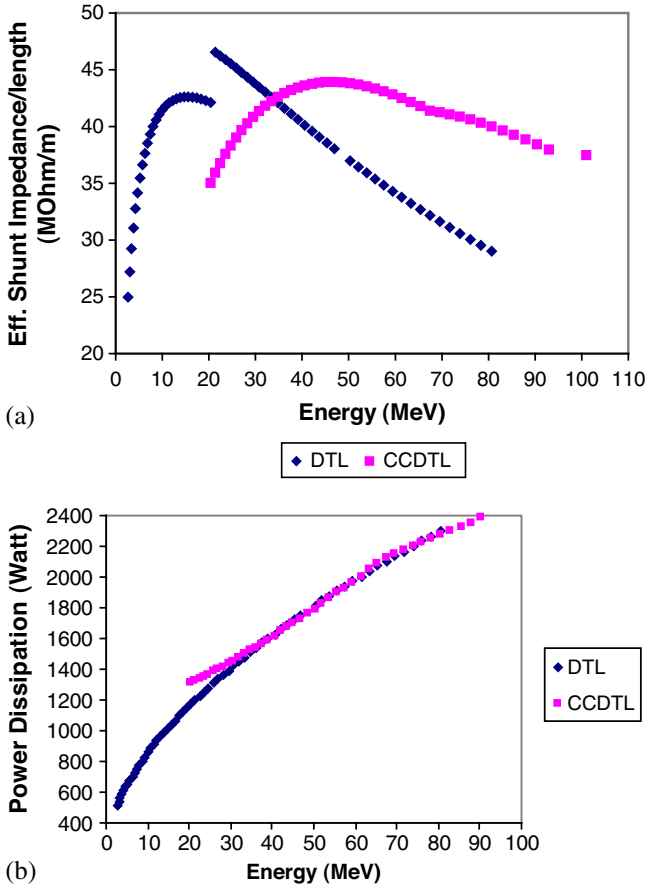

Figure 2. Variation of (**a**) the effective shunt impedance and (**b**) power dissipation in the CCDTL and DTL cavities with energy.

Table 2. Parameters of DTL and CCDTL.

Parameter		DTL	CCDTL
Energy range (MeV)		3–40.12	40.12–100.25
Frequency (MHz)		352.21	704.42
Current (mA)		28.8	28.8
Focussing lattice		FFDD	FD
Lattice period		$4\beta\lambda$	$5\beta\lambda$
Quadrupole gradient (T/m)		43	39.8–18.03
Eff. length of quad. (cm)		4.72	8.0
No. of quadrupoles		146	186
Synchronous phase (deg)		-30	-30
Avg. acc. gradient (MV/m)		2.5	1.04–2.5
Aperture radius (cm)		1.0	1.2
Total length (m)		28	69.5
Norm. rms trans. emitt. (π cm-mrad)	x	0.0228–0.0231	0.0231–0.0233
	y	0.0227–0.0236	0.0236–0.0242
Long. emitt. (deg-MeV)		0.104–0.115	0.115–0.236

At 100 MeV, superconducting elliptical cavities at 704.42 MHz are used to accelerate the beam to 1 GeV. The advantages of switching over to superconducting technology are two-fold: high RF efficiency, which is important for CW operations, and large apertures, which can minimize particle loss [13].

The cavities are designed to perform over a given velocity range and are identified by a design velocity called the geometric velocity or β_G. The design approach takes advantage of the large velocity acceptance of the superconducting cavities. For a cavity with N identical cells, the transit time factor T can be expressed as a product of two separate factors $T = T_G T_S$. The gap factor T_G, which is also the transit-time factor for a single gap of length g, RF wavelength λ, and particle-velocity β, is given by the expression

$$T_G = \sin(\pi g/\beta\lambda)/(\pi g/\beta\lambda).$$

The synchronism factor T_S is a function of N and of the ratio of the local velocity, β, to the cavity geometric velocity, $\beta_G = 2L/\lambda$, where L is the cell length. The synchronism factor is given by

$$T_S = \left\{ \begin{array}{l} (-1)^{(N-1)/2} \cos(N\pi\beta_G/2\beta)/N\cos(\pi\beta_G/2\beta), \ N \text{ odd} \\ (-1)^{(N/2)+1} \sin(N\pi\beta_G/2\beta)/N\cos(\pi\beta_G/2\beta), \ N \text{ even} \end{array} \right\}.$$

In order to choose the number of cells per cavity, a compromise has to be made between many competing effects. SUPERFISH [14] is used to compute the gap factor T_G and the synchronism factor T_S is computed from the above expression for varying number of cells per cavity. The total transit time factor vs. the energy is plotted in figure 3. As can be seen in the figure a small number of cells per cavity provides a large velocity acceptance. On the other hand, using a larger number of cells per cavity has the advantage of reducing the overall number of system components, system size and system complexity. As a compromise between the two, in our design, we have chosen five cells per cavity.

Once the number of cells per cavity has been chosen, in order to efficiently design a Linac it is necessary to divide it in sections, each using a different cavity geometry in a

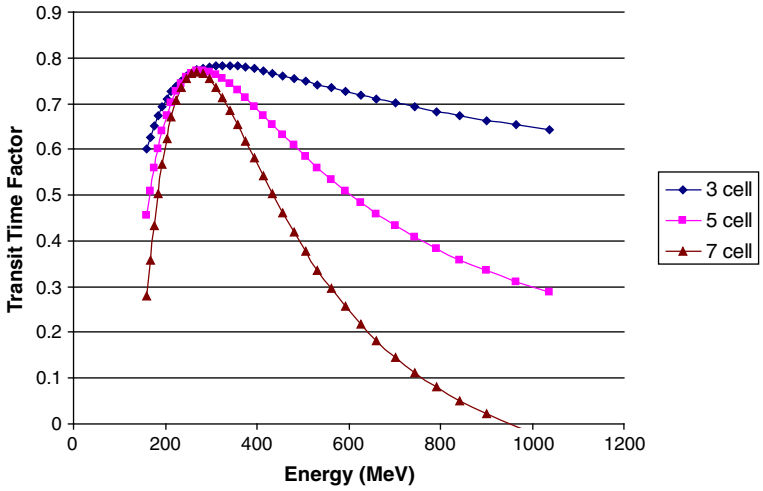

Figure 3. Variation of TTF with energy for different number of cells/cavity.

given energy range. To begin with, the β_G values for the cavities, the number of constant β_G sections and the beam velocity limits for each section have to be determined. In this design the minimum transit time factor for a given cavity of N cells has been kept at least 75% of the maximum value. Based on this velocity acceptance limit, the entire energy range from 100 MeV to 1 GeV is divided into three sections of constant β cavities as shown in figure 4.

The superconducting Linac accelerates the beam using three different types of 5-cell elliptical cavities designed corresponding to geometric beta values $\beta_G = 0.49$, 0.62 and 0.80. The next step in the Linac design is to determine the accelerating gradient. The operating gradient is chosen such that it limits the peak surface magnetic field below 70 mT and a peak surface electric field less than 27.5 MV/m to avoid the risk of field emission.

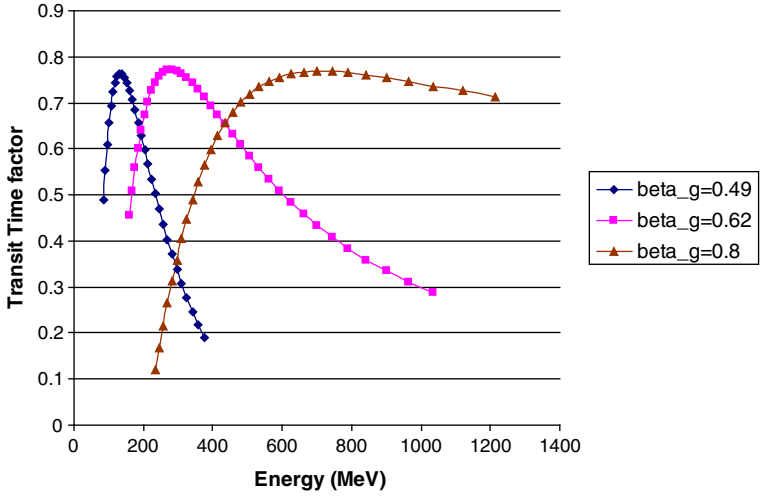

Figure 4. Variation of the TTF of the designed elliptic cavities with energy.

With this criterion, the maximum accelerating gradient comes out to be 11 MV/m for $\beta_G = 0.49$ cavities and 15 MV/m for $\beta_G = 0.62$ and $\beta_G = 0.8$ cavities.

The transverse focussing in the superconducting Linac is achieved using room-temperature electromagnetic quadrupole doublets in between the cryomodules containing the superconducting cavities. The focussing doublets are placed after every two cavities in the first section, which will have 16 cryostats, after every three cavities in the second section having 15 cryostats and after every four cavities in the third section having 17 cryostats. To obtain a current independent match between the normal conducting Linac and superconducting Linac, which has a weaker focussing, the quadrupole gradients in the CCDTL are gradually reduced with energy. Transverse matching is done using the last two quadrupoles in the CCDTL and the first two quadrupoles in the superconducting Linac. Transverse matching between two superconducting sections was done by making small adjustments to the quadrupole gradients at the transition between the sections. Longitudinal matching was achieved by adjusting the synchronous phase ϕ_s in the superconducting cavities to maintain constant longitudinal phase advance per unit length on both sections and maintaining a constant energy gain in each cavity. This was done by keeping $(\Delta W \tan \phi_s/L)$ constant on both sides of the transition, where ΔW is the energy gain per cryomodule and L is the length of the focussing period. The main parameters of the superconducting Linac are given in table 3.

3. Beam dynamics

The computer code PARMILA [15] was used to do the end-to-end beam dynamics simulations from 3 MeV to 1 GeV. Figure 5 shows the x, y and phase profiles of the beam from the DTL through the superconducting Linac for a beam current of 28.8 mA. The variation

Table 3. Parameters of the superconducting Linac.

Parameter		$\beta_G = 0.49$	$\beta_G = 0.62$	$\beta_G = 0.80$
Energy range (MeV)		100.25–191.62	191.62–434.88	434.88–1014.26
Frequency (MHz)		704.42	704.42	704.42
Current (mA)		28.8	28.8	28.8
Acc. gradient (MV/m)		11	15	15
Trans. focussing lattice		Doublet	Doublet	Doublet
Lattice period (cm)		308.13	607.90	793.41
Quad. gradient (T/m)		5.8–4.308	4.5	4.4
Eff. length of quad. (cm)		35	40	45
Cavities/cryomodule		2	3	4
No. of cryomodules		16	15	17
Aperture radius (cm)		4.0	4.0	4.0
Total RF power (MW)		2.63	7.01	16.69
Total length (m)		49.3	91.19	134.88
Norm. rms trans. emitt. (π cm-mrad)	x	0.0233–0.0255	0.0255–0.026	0.026–0.031
	y	0.0242–0.0245	0.0245–0.026	0.026–0.026
Long. emittance (deg-MeV)		0.236–0.248	0.248–0.271	0.271–0.279

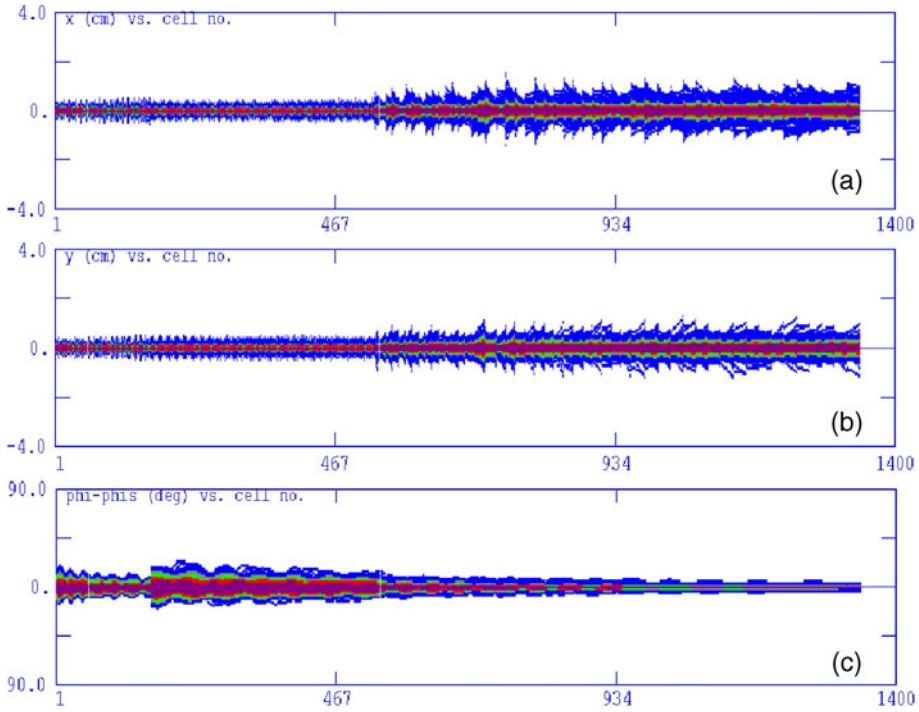

Figure 5. Evolution of the beam sizes **(a)** in x, **(b)** in y and **(c)** longitudinal phase, as a function of cell number.

of maximum beam size with energy is shown in figure 6. As can be seen from the figure, the maximum beam radius never exceeds 8 mm in the Linac. The beam transmission is 100% from 3 MeV to 1 GeV.

4. Summary and conclusions

A Linac-based accelerator has been designed for the Indian ADS programme and its beam dynamics studies have been done. The total length of the designed accelerator is about 380 m and the overall transmission is about 96%. The 4% loss takes place in RFQ during bunching of the beam which is not expected to pose any radiation problem. A 30 mA, 20 MeV CW proton Linac, consisting of RFQ and DTL accelerating structures, is already under construction at BARC, India as an injector to the 1 GeV Linac for ADS.

Acknowledgements

The authors thank Drs S Banerjee and R K Sinha for their keen interest and support for these studies. The authors also thank Drs A Kakodkar and V C Sahni for useful discussions for this work.

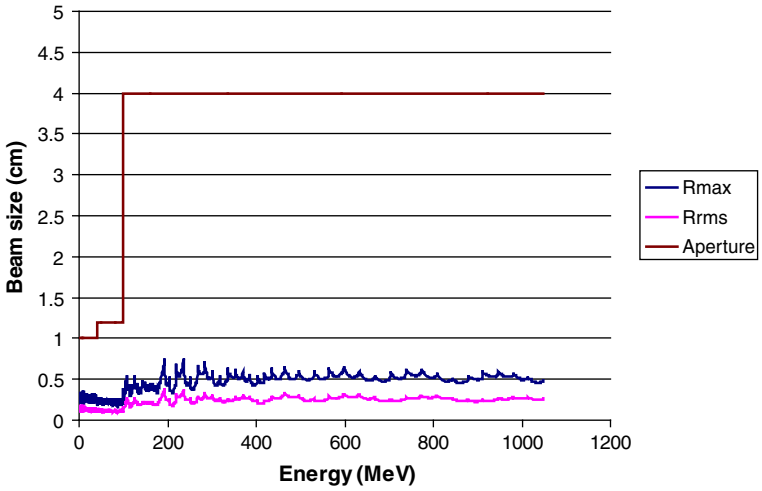

Figure 6. Variation of beam size with energy in the Linac.

References

[1] F Carminati, R Klapisch, J P Revol, J A Rubio and C Rubbia, CERN/AT/93-47(ET) C Rubbia *et al*, CERN/AT/95-44 (ET); CERN/LHC/96-01 (EET); CERN/AT/95-53 (ET); CERN/LHC/97-01 (EET)

[2] S S Kapoor, *Roadmap for development of accelerator-driven sub-critical reactor systems*, BARC/2001/R/004

[3] S Henderson, Spallation neutron source progress, challenges and power upgrade paths, *Proceedings of EPAC08*, Genoa, Italy, http://accelconf.web.cern.ch/AccelConf/e08/papers/thxg01.pdf

[4] John W Staples, *AIP Conf Proc.* **249**, 1483 (1992)

[5] M Weiss, Radio frequency quadrupole, *Proc. CAS* (Aarhus, Denmark, 1986); CERN 87-10 (1987)

[6] J H Billen, F L Krawczyk, R L Wood and L M Young, *Proceedings of the 1994 International Linac Conference*, Vol. 1, p. 341

[7] T P Wangler, *Principles of RF linear accelerators* (John Wiley & Sons Inc., 1998)

[8] K Shepard *et al*, *Proceedings of the XIX International Linac Conference* (Chicago, Illinois) p. 956

[9] C Pagani *et al*, Design criteria for elliptical cavities, SRF, 2001

[10] P Singh, S V L S Rao, Rajni Pande, T Basak, Shweta Roy, M Aslam, P Jain, S C L Srivastava, Rajesh Kumar, P K Nema, S Kailas and V C Sahni, *Pramana – J. Phys.* **68**, 33 (2007)

[11] R S Mills, K R Crandall and J A Farrell, Designing Self-Matching Linacs, *Proc. 1984 Linac Conf.*

[12] S V L S Rao and P Singh, *Pramana – J. Phys.* **74**, 247 (2010)

[13] H Padamsee *et al*, *RF superconductivity for accelerators*, Cornell University, Ithaca, New York (Wiley-Interscience Publication, 1998)

[14] J H Billen and L M Young, POISSON SUPERFISH, LA-UR-96-1834, L.A.N.L. K.R. Crandall, TRACE 3D Documentation, Third edition Los Alamos Report LA-UR-97-886, May 1997

[15] J H Billen, *PARMILA* Code, LA-UR-98-4478, Revised July 26, 2005